Cent. Eur. J. Chem. • 9(3) • 2011 • 379-385
DOI: 10.2478/s11532-011-0018-6

VERSITA

Central European Journal of **Chemistry**

Two staged pattern formation and spontaneous wave breakup in the ferroin-bromate-pyrocatechol reaction

Invited Paper

Mohammad Harati, Jichang Wang*

Department of Chemistry and Biochemistry,
University of Windsor, Windsor ON N9B 3P4, Canada

Received 22 November 2010; Accepted 24 January 2011

Abstract: This report investigated nonlinear spatiotemporal behavior in the ferroin-bromate-pyrocatechol reaction, in which two stages of wave formation, separated by several hours of quiescent period, were observed. In addition to its great photosensitivity, the second stage wave activity could undergo spontaneous breakups at broad reaction conditions. Analysis based on one-dimensional space-time plot suggests that the breakup was caused by propagation slowdown of the leading wave. Due to the presence of coupled autocatalytic reactions, the propagation of the initial and the second stage waves exhibited different and subtle responses to the variation of the concentration of each reagent.

Keywords: *Chemical waves • Coupled autocatalytic reactions • Nonlinear reaction dynamics • Photochemistry*

1. Introduction

Pattern formation in spatially extended media is an important subject in nonlinear dynamics, which has been frequently encountered in nature [1-20]. In chemistry, when a nonlinear reaction system is coupled with molecular transportations, various spatial structures may emerge, where the relative diffusivity of activator and inhibitor has a significant role in determining chemical wave formation [1-12]. For example, in order to obtain Turing patterns the inhibitor must diffuse significantly faster than activator [21]. Transitions from regular to complicated spatiotemporal behavior could also take place via manipulating the underlying dynamics. Indeed, there have been increasing interests in the study of pattern formation in perturbed media, where either the local or global nonlinear dynamics was subjected to various types of forcing [22-27]. Numerous interesting behaviors which do not exist in perturbation-free media have been observed.

Among a great number of reports highlighting the importance of temporal dynamics in pattern formation [28-30], Park and Lee demonstrated in the Belousov-Zhabotinsky (BZ) experiments in an open flow reactor the presence of synchronization defect lines where the phase of the local orbit of a spiral wave changed by multiples of 2π due to period-doubling dynamics [28]. To explore novel chemical wave formation, we have recently engaged in developing new chemical oscillators that could exhibit complex nonlinear dynamics. The research was primarily carried out via introducing a second substrate such as hydroquinone or 1,4-cyclohexanedione (CHD) into the ferroin-BZ reaction, in which coupled autocatalytic feedbacks are implemented [31-33]. Those studies have shown that sequential oscillations in a stirred system might lead to sequential pattern formation in a spatially extended medium [34]. If the quiescent period was within a moderate range, locally emerged unexcitable regions caused the breakup of existing waves, which consequently led to complicated spatiotemporal structures [35].

In this report, we investigated pattern formation in a thin layer of ferroin-bromate-pyrocatechol reaction solution. In comparison to the uncatalyzed bromate-pyrocatechol reaction, the presence of ferroin not only provides observable periodic color changes, but also implements coupled nonlinear feedbacks *via* reacting with bromine dioxide radicals [36-38]. As presented in

---

* E-mail: jwang@uwindsor.ca

the following, the ferroin-bromate-pyrocatechol system produced two staged pattern formation and chemical waves that underwent spontaneous breakups, leading to the formation of complex spatial temporal structures.

2. Experimental Procedure

Stock solutions of $NaBrO_3$ (Aldrich, 99%), 0.6 M, and sulfuric acid (Aldrich, 95-98%), 4.0 M, were prepared with doubly distilled water. Ferroin, 0.025 M, was prepared from a calculated amount of $FeSO_4$•$7H_2O$ (Aldrich, 99+%) and 1,10-phenanthroline (Aldrich, 99+%). Pyrocatechol (Sigma, 99%) was directly dissolved in the reaction mixture. The reaction solution was prepared by mixing all reagents in a stirred batch reactor, where the reaction was allowed, depending on the specific study of wave formation, to evolve for a certain period of time. Chemical waves were investigated by spreading the reaction solution into a thin layer (0.5 mm) between two microscope slides. To examine whether three dimensional (3D) effects played a role in the spontaneous breakups, experiments have been repeated with 0.3 mm thick solution layer and qualitatively the same results were achieved.

Throughout this research, evolution of the spatially extended medium took place at room temperature (21 ± 1^{o}C) and was monitored with a CCD camera equipped with a zoom lens. The CCD camera was connected to a personnel computer running a frame grabber program (Matrox Imaging Library). The perturbation of light was performed with a halogen lamp equipped with dual bifurcated optic fibers (Fisher Scientific, Model DLS-100HD, 150 mW cm^{-2}). A local perturbation was implemented by placing one fiber on top of the microscope slide.

3. Results and Discussion

3.1. Two staged pattern formation

Fig. 1 presents four snapshots recorded at (a) 5, (b) 145, (c) 181, and (d) 230 seconds after setting up the thin layer. Here, the reaction solution was prepared in a stirred batch reactor with [pyrocatechol] = 0.095 M, $[BrO_3^-]$ = 0.125 M, $[H_2SO_4]$ =1.4 M, and [ferroin] = 3.0×10^{-3} M,and the mixture was quickly injected into the thin layer. After a brief induction time, oxidation waves with a light green color emerged at the boundaries as shown in Fig. 1b. While these initial waves were propagating in space, the rest of the medium turned into red color, which indicated that the initial state (brown color in Fig. 1a) was a metastable state. As shown in Fig. 1c, oxidation waves also emerged at the centre of the medium. The above wave activities lasted for about 300 s, then the whole medium turned into a homogeneous state again. Notably, the homogeneous state could last for more than 12 hours (*i.e.*, quiescent time) before spontaneous wave formation took place again. Waves developed beyond 12 hours are referred as the second stage wave activity throughout this study.

Our study indicated that the quiescent time period was greatly reduced by letting the reaction solution evolve in a stirred batch reactor. The second stage wave activity presented in Fig. 2 was achieved by keeping the reaction solution in a stirred system for 50 min. The four snapshots were recorded at (a) 120, (b) 154, (c) 224, and (d) 305 min after spreading the solution into the thin slab, respectively. Fig. 2a indicates that the initial state was an oxidized state. In Fig. 2b reduction waves emerged spontaneously at numerous locations. These reduction waves gradually developed into oxidation waves as seen in Figs. 2c,2d. The second stage waves continued for several hours, which is significantly longer than those initial waves.

3.2. Photosensitivity

The study of perturbed spatiotemporal dynamics has attracted increasing attention in the last two decades [21-26], in which photosensitive chemical oscillators have become desired model systems since photosensitivity provided a convenient approach of implementing various spatial-temporal perturbations. Preliminary studies presented in Fig. 3 showed that waves in the ferroin-bromate-pyrocatechol system are also photosensitive. Fig. 3a is a snapshot taken right before illumination. As shown in Fig. 3b, which was taken right after illuminating the medium for 1 min with a beam of halogen light of the intensity 50 mW cm^{-2}, light quenched local wave activities. After a brief transient time, the illuminated area became a nucleation center emitting new wave activities. This result suggests that the chemical system studied here may be employed as a model system to explore perturbed nonlinear spatiotemporal dynamics.

3.3. Spontaneous wave breakup

Fig. 4 presents the second stage wave activity recorded at (a) 152, (b) 157, (c) 169, (d) 182, (e) 189, and (f) 207 min after setting up the thin layer. Here the reaction conditions were [pyrocatechol] = 0.091 M, $[BrO_3^-]$ = 0.125 M, $[H_2SO_4]$ = 1.30 M, and [ferroin] = 3.0×10^{-3} M. Note that the reaction was first allowed to evolve in a stirred batch reactor for 50 min and no temporal oscillations was observed during

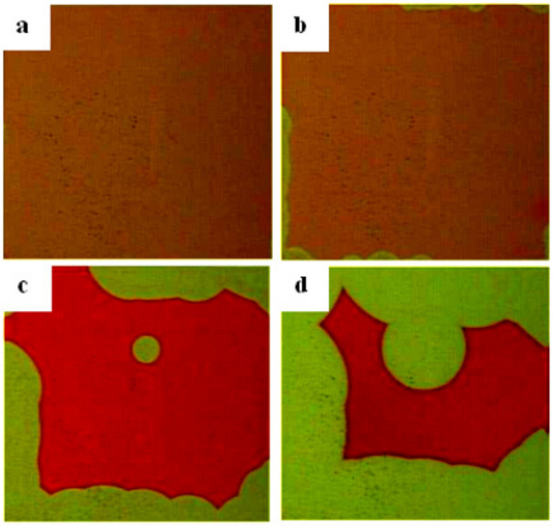

Figure 1. Snapshots of the first stage wave activity recorded at: (a) 5, (b) 145, (c) 181, and (d) 230 s after setting up the reaction-diffusion medium. The initial concentrations are [pyrocatechol] = 0.095 M, [BrO_3^-] = 0.125 M, [H_2SO_4] =1.4 M, and [ferroin] = 3.0×10^{-3} M. The size of the medium is 39 mm × 41 mm.

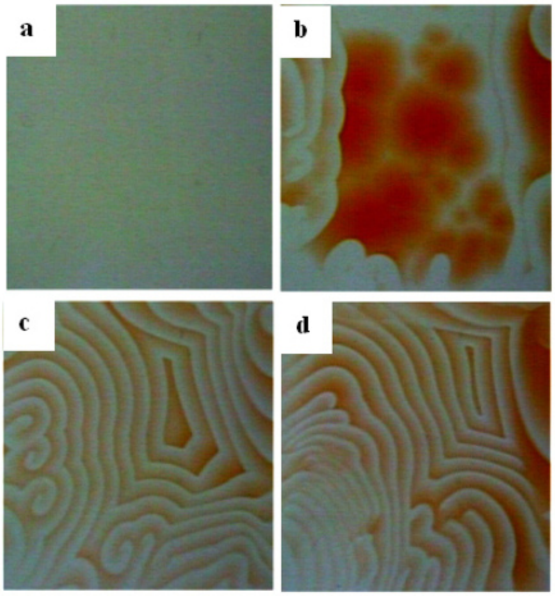

Figure 2. Snapshots of the second stage wave activity recorded at: (a) 120, (b) 154, (c) 224, and (d) 305 min after setting up the reaction-diffusion medium. The initial concentrations are [pyrocatechol] = 0.085 M, [BrO_3^-] = 0.125 M, [H_2SO_4] = 1.4 M, and [ferroin] = 3.0×10^{-3} M. The size of the medium is 39 mm × 41 mm.

such a period. Figs. 4a and 4b show that as the wave front propagated downward from the top boundary, the distance between consecutive fronts decreased and eventually wave segments came to direct front-to-back collision, causing wave breakups in Fig. 4c. More complicated spatial structures were gradually developed in Fig. 4f as a result of consecutive breakups. Similar scenario of spontaneous wave breakup could also be seen at the bottom corners. Notably, the breakup did not involve any external disturbance; rather it arose from the natural evolution of the system.

To shed light on how the front-to-back collision occurs, Fig. 5 presents one-dimensional (1D) space-time plots of the reaction-diffusion medium studied in Fig. 4. The space-time plot in Fig. 5a was produced *via* piling the 1D frames recorded along the vertical dashed line indicated in Fig. 4d. Since the horizontal direction represents space and the time going upward, the slope of these 1D pulses represents wave propagation velocity with that the larger the slope, the slower the wave propagates. Fig. 5a shows that as pulses propagated from the left edge into the medium (*i.e.*, waves from the top edge of the 2D images in Fig. 4), their velocity decreased. The deceleration in wave propagation resulted in the following pulse run into the preceding one, exhibiting transient packing phenomenon. There was a region where wave propagation decreased more rapidly, causing the breakup to take place there. Different from the packing behaviour of wave trains reported in the ferroin-bromate-CHD medium in capillary tubes [39,40], here it occurred as a result of the slow down of the preceding wave activity rather than the repelling effect when it approached to the leading pulse. It is important to point out that the ferroin-bromate-CHD reaction also consists of coupled autocatalytic cycles. Thus, the interesting spatiotemporal behaviour seen here may be the result of coupled autocatalytic cycles.

Fig. 5b is a space-time plot of the wave activity collected across the horizontal line (dotted line) in Fig. 4d. This plot confirms that during the initial stage regular fronts propagated through this location. Upon the occurrence of wave breakups, irregular spatiotemporal behaviour emerged. In this ferroin-bromate-pyrocatechol system, the above breakup behaviour could be readily achieved, especially at low concentrations of bromate and/or sulphuric acid.

3.4. Wave propagation at different reaction conditions

Figs. 6-9 plot the wave propagation rate versus the concentration of each reagent. For the initial waves, the analysis of propagation velocity was carried out soon after waves appeared in the medium. For the second stage waves, there was an apparent decrease in the propagation velocity as time evolved, all the following propagation rates were measured at 30 min after the appearance of the first wave activity. Fig. 6 shows that the propagation rate of both the initial and second

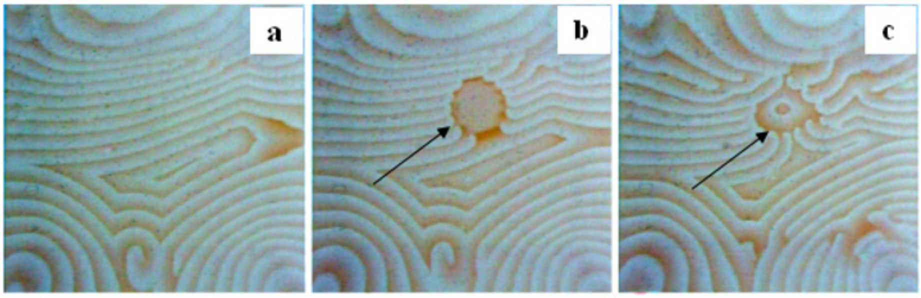

Figure 3. Photosensitivity of the second stage waves. Snapshots were taken at (a) 1 minute before illumination, (b) 1, and (c) 12 min after removing light illumination. Composition of the system is [pyrocatechol] = 0.091 M, [BrO_3^-] = 0.15 M, [H_2SO_4] = 1.4 M, and [ferroin] = 3.0×10^{-3} M. The arrow indicates where the local illumination was applied.

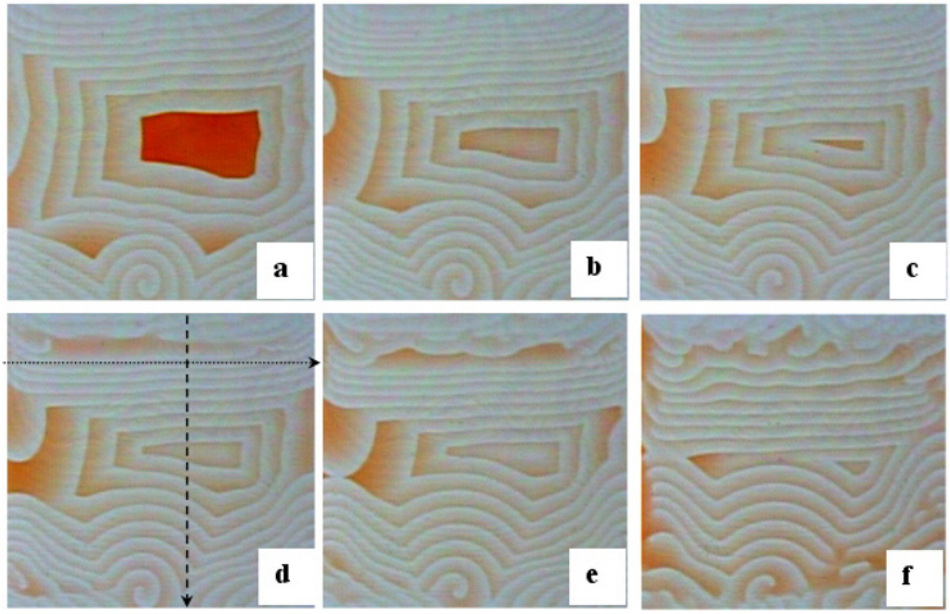

Figure 4. Snapshots showing the spontaneous breakups of chemical waves were recorded at: (a) 152, (b) 157, (c) 169, (d) 182, (e) 189, and (f) 207 min after spreading solution into the thin layer between two microscopic slides. The initial reaction conditions are [pyrocatechol] = 0.091 M, [BrO_3^-] = 0.125 M, [H_2SO_4] = 1.3 M, and [ferroin] = 3.0×10^{-3} M. The size of the medium shown here is 43 × 47 mm.

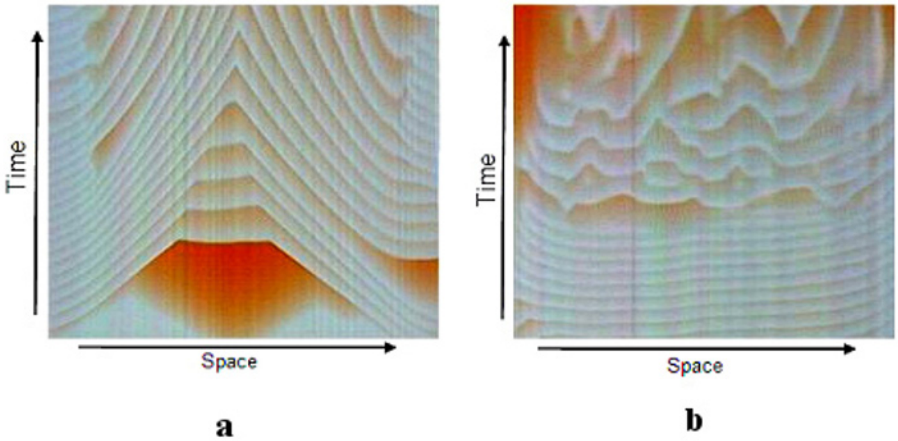

Figure 5. One-dimensional space-time plots showing the evolution of waves at: (a) the location indicated by the dashed line, and (b) the location indicated by the dotted line in Fig. 4d. The time interval presented here is 115 min. The direction of space matches the arrows in Fig. 4d.

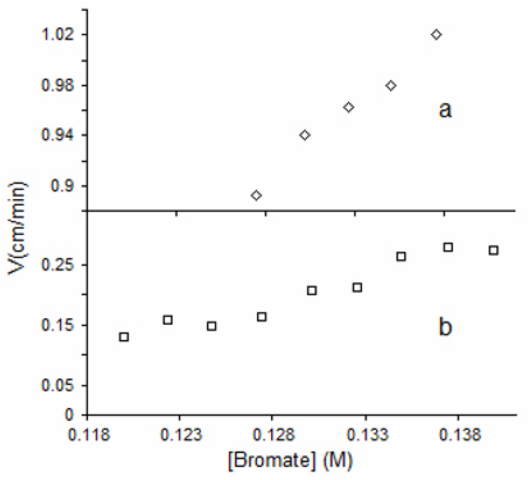

Figure 6. Propagation rate of (a) initial waves and (b) second stage waves as a function of bromate concentration. Other reaction conditions are [pyrocatechol] = 0.091 M, $[H_2SO_4]$ = 1.4 M and [ferroin] = 3.0×10^{-3} M;

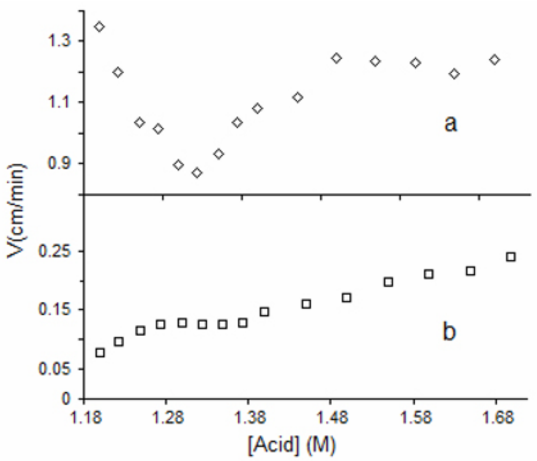

Figure 7. Propagation rate of (a) initial waves and (b) second stage waves as a function of acid concentration. Other reaction conditions are [pyrocatechol] = 0.091 M, $[BrO_3^-]$ = 0.125 M and [ferroin] = 3.0×10^{-3} M.

stage waves increased with the bromate concentration. This is consistent with the fact that higher bromate concentration favours, the production of autocatalyst $HBrO_2$, which is a key factor in determining chemical wave velocity. For bromate concentration lower than 0.11 M, no wave activity could be achieved. For the initial waves, when bromate concentration was lower than 0.124 M, the propagating fronts were rapidly overwhelmed by simultaneous appearance of a large number of excitation sites. As a result, no wave velocity was determined there. Notably, bromate concentration has the same influence on wave propagation in both stages, indicating that bromate has a consistent role throughout the reaction process.

Fig. 7 plots wave propagation rate as a function of acid concentration, where no wave activity was obtained for the acid concentration higher than 1.70 M or lower than 1.20 M. This plot shows that while the velocity of the second stage waves increased steadily with acid concentration, the velocity of initial waves varied in a complicated fashion. It followed a semi-circular way at low acid concentration range and then became nearly constant with the further increase of acid concentration. Such subtle influence of acid concentration on wave speed may be understood from the following: In the pyrocatechol system there are two paths for the autocatalytic production of $HBrO_2$ (*i.e.*, reactions (1)+(3) or (2)+(3)):

$$H_2Q + 2BrO_2^{\cdot} \rightarrow 2HBrO_2 + Q \tag{1}$$

$$Fe(phen)_3^{2+} + BrO_2^{\cdot} + H^+ \rightarrow HBrO_2 + Fe(phen)_3^{3+} \tag{2}$$

$$BrO_3^- + HBrO_2 + H^+ \rightarrow 2BrO_2^{\cdot} + H_2O \tag{3}$$

in which the acid H^+ only participated in one of the above two paths ((2)+(3)). The complicated dependence on H^+ suggests that both of the above autocatalytic cycles played an active role in the formation of initial waves. As the acid concentration increased gradually, however, the path of (2)+(3) became the dominant one. This conclusion is consistent with the observation that there was a stronger color change between red (ferroin) and blue (ferriin) at higher acid concentration.

Since pyrocatechol also participated one of the above two autocatalytic paths (steps (1)+(3)), one may expect pyrocatechol concentration to exhibit subtle influences on the wave propagation rate as well. It is indeed the case as plotted in Fig. 8, where both the initial and second stage waves exhibited great response to variation of pyrocatechol concentration. This further highlights that pyrocatechol is different from an ordinary substrate used in the classic BZ reaction [41,42]. Fig. 9 illustrates that the initial and second stage waves exhibited opposite responses to the variation of ferroin concentration. The opposite dependence of wave propagation on ferroin is most likely due to the evolution of the underlying nonlinear dynamics, in which the continuous consumption of pyrocatechol allowed the autocatalytic process of (2)+(3) to become the dominated one at the second stage. According to our observation, high ferroin concentration favoured the occurrence of multiple nucleation sites in the initial stage, but reduced the lifetime of those chemical waves.

Earlier studies reported that wave velocity in the BZ reaction depended strongly on H_2SO_4 and bromate concentrations and the form of the concentration dependence was the square root of the product of acid and bromate [41-45]. When our results were analyzed

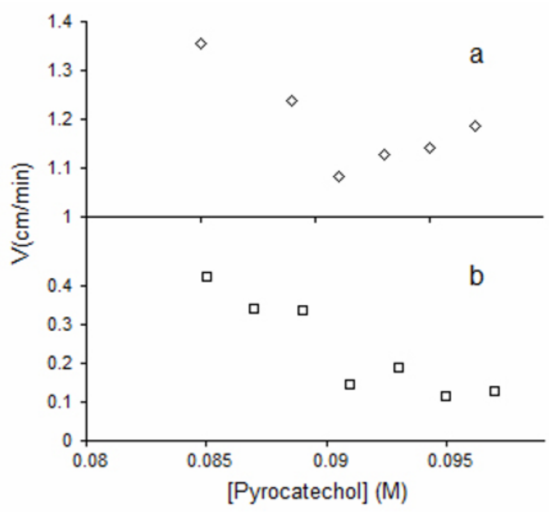

Figure 8. Propagation rate of (a) initial waves and (b) second stage waves as a function of pyrocatechol concentration. Other reaction conditions are $[BrO_3^-]$ = 0.1248 M, $[H_2SO_4]$ = 1.4 M and [ferroin] = 3.0×10^{-3} M.

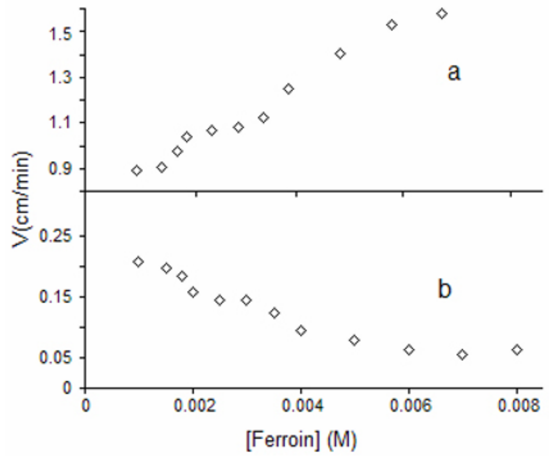

Figure 9. Propagation rate of (a) initial waves and (b) second stage waves as a function of ferroin concentration. Other reaction conditions are [pyrocatechol] = 0.091 M, $[BrO_3^-]$ = 0.125 M and $[H_2SO_4]$ = 1.4 M.

in such a square root form, the best fit for the data was v(cm/min) = $0.2594\times([H_2SO_4][BrO_3^-])^{1/2} + 0.1342$ with a linear correlation coefficient of 0.876. When attempted to fit the data with $[H_2SO_4][BrO_3^-]$, the linear correlation coefficient became 0.871, only slightly worse. The deviation from the relationship found in the classic BZ reaction is most likely due to that the autocatalytic generation of $HBrO_2$ in this ferroin-bromate-pyrocatechol system is not a simple process. Competitions between paths (1)+(3) and (2)+(3) complicates the dependence of wave velocity on initial compositions.

4. Conclusions

This research investigated nonlinear spatiotemporal behaviour in the ferroin-bromate-pyrocatechol system and observed two staged pattern formation, in which short lived, fast propagating wave activity developed shortly after mixing all reagents together. Based on the reaction kinetics investigated earlier in the stirred system [37], the ferroin-catalyzed bromate-pyrocatechol system exhibits only one oscillation window with a very long induction time (> 8000 s). The medium shall therefore be at an excitable state when those initial waves are developed. The long quiescent time period during which the medium does not produce any wave activity corresponds to the long induction time observed in the stirred medium. As the system evolves toward the oscillation window, the excitability of the reaction-diffusion medium increases and eventually reaches a point where propagating waves could be initiated and sustained. In other words, the second stage waves seen above might have started emerging while the system was still outside the oscillation window (*i.e.*, excitable).

In addition to their great photosensitivity, the second stage waves may undergo spontaneous breakups, resulting in irregular spatiotemporal structures. The breakup appeared to be due to significant changes in wave propagation velocity, where the following waves run into the preceding one. Similar sequential wave formation and anomalous dispersion relationship have been reported earlier in bromate-based chemical oscillators [34,39]. The fact that all those bromate systems consist of coupled autocatalytic processes suggests that the coupled nonlinear feedbacks are likely responsible for the emergence of those interesting behaviour in this pyrocatechol system and represent an effective way of inducing novel chemical wave formation.

Acknowledgements

This research was supported by Natural Sciences and Engineering Research Council of Canada (NSERC), and Canada Foundation for Innovation (CFI).

References

[1] R.J. Field, M. Burger (Eds.), Oscillations and Traveling Waves in Chemical Systems (Wiley-Interscience, New York, 1985)
[2] A.T. Winfree, The Geometry of Biological Time (Springer, Heidelberg, 2000)
[3] S.K. Scott, Chemical Chaos (Oxford University Press, New York, 1994)
[4] B.R. Johnson, S.K. Scott, A.F. Taylor, J. Chem. Soc. Faraday Trans. 93, 3733 (1997).
[5] C. Luengviriya, U. Storb, G. Lindner, S.C. Müller, M. Bar, M.J.B. Hauser, Phys. Rev. Lett. 100, 148302 (2008)
[6] V.K. Vanag, I. Hanazaki, J. Phys. Chem. A 101, 2147 (1997)
[7] T.R. Chigwada, P. Parmananda, K. Showalter, Phys. Rev. Lett. 96, 244101 (2006)
[8] C. Luengviriya, U. Storb, M.J.B. Hauser, S.C. Müller, Phys. Chem. Chem. Phys. 8, 1425 (2006)
[9] A.L. Kawczynski, J. Non-Equilib. Thermodyn. 3, 29 (1978)
[10] L. Adamčíková, Z. Farbulová, P. Ševčík, New J. Chem. 25, 487 (2001)
[11] I. Szalai, K. Kurin-Csörgei, M. Orbán, Phys. Chem. Chem. Phys. 4, 1271 (2002)
[12] O. Steinbock, S.C. Müller, Phys. Rev. E 47, 1506 (1993)
[13] E. Fung, W.W. Wong, J.K. Suen, T. Bulter, S. Lee, J.C. Liao, Nature 435, 118 (2005)
[14] K. Horikawa, K. Ishimatsu, E. Yoshimoto, S. Kondo, H. Takeda, Nature 441, 719 (2006)
[15] W.W. Wong, T.Y. Tsai, J.C. Liao, Mol. Syst. Biol. 3, 1 (2007)
[16] B. Blasius, A. Huppert, L. Stone, Nature 399, 354 (1999)
[17] S. Danø, P. Sørensen, F. Hynne, Nature 402, 320 (1999)
[18] T. Hideshima, Y. Kato, Biophys. Chem. 124, 100 (2006)
[19] P. Mohanty, Nature 437, 325 (2005)
[20] N.J. Abram, M.K. Gagan, Z. Liu, W.S. Hantoro, M.T. McCulloch, B.W. Suwargadi, Nature 445, 299 (2007)
[21] K. Showalter, R. Kapral (Eds), Chemical Wave and Pattern Formation (Kluwer Academic Publishers, Dordrecht, 1995)
[22] O. Steinbock, V. Zykov, S.C. Müller, Nature 366, 322 (1993)
[23] V. Petroy, Q. Ouyang, H. Swinney, Nature 388, 655 (1997)
[24] S. Kádár, J. Wang, K. Showalter, Nature 391, 770 (1998)
[25] L. Kuhnert, K.I. Agladze, V.I. Krinsky, Nature 337, 244 (1989)
[26] J. Wang, S. Kádár, P. Jung, K. Showalter, Phys. Rev. Lett. 82, 855 (1999)
[27] L. Yang, I.R. Epstein, J. Phys. Chem. A 106, 11676 (2002)
[28] J.S. Park, S.J. Woo, K.J. Lee, Phys. Rev. Lett. 93, 098302 (2004)
[29] A. Goryachev, H. Chate, R. Kapral, Phys. Rev. Lett. 80, 873 (1998)
[30] Q. Ouyang, J. M. Flesselles, Nature 379, 143 (1996)
[31] J. Zhao, Y. Chen, J. Wang, J. Chem. Phys. 122, 114514 (2005)
[32] Y. Chen, J. Wang, J. Phys. Chem. A 109, 3950 (2005)
[33] N. Li, J. Zhao, J. Wang, J. Chem. Phys. 128, 244509 (2008)
[34] S. Shah, J. Wang, J. Phys. Chem. C 111, 10639 (2007)
[35] V. Ruisi, J. Wang, Phys. Rev. E 78, 016102 (2009)
[36] M. Harati, J. Wang, Z. Phys. Chem. 222, 997 (2008)
[37] M. Harati, J. Wang, J. Phys. Chem. A 112, 4241 (2008)
[38] P. Herbine, R. J. Field, J. Phys. Chem. 84, 1330 (1980)
[39] N. Manz, S.C. Müller, O. Steinbock, J. Phys. Chem. A 104, 5896 (2000)
[40] C.T. Hamik, N. Manz, O. Steinbock, J. Phys. Chem. A 105, 6144 (2001)
[41] L. Kuhnert, H.J. Krug, J. Phys. Chem. 91, 730 (1987)
[42] R.J. Field, R.M. Noyes, J. Am. Chem. Soc. 96, 2001 (1974)
[43] Z. Nagy-Ungvarai, J.J. Tyson, B. Hess, J. Phys. Chem. 93, 707 (1989)
[44] P.M. Wood, J. Ross, J. Chem. Phys. 82, 1924 (1985)
[45] K. Showalter, J. Phys. Chem. 85, 440 (1981)
[46] M. Harati, J. Wang, Chaos 19, 023116 (2009)